

## Polarized light microscopy of chemical-vapor-deposition-grown graphene on copper

K. Kertész, A. A. Koós, A. T. Murdock, Z. Vértesy, P. Nemes-Incze et al.

Citation: *Appl. Phys. Lett.* **100**, 213103 (2012); doi: 10.1063/1.4719205

View online: <http://dx.doi.org/10.1063/1.4719205>

View Table of Contents: <http://apl.aip.org/resource/1/APPLAB/v100/i21>

Published by the [American Institute of Physics](http://www.aip.org).

---

### Related Articles

Using carbon chains to mediate magnetic coupling in zigzag graphene nanoribbons

*Appl. Phys. Lett.* **100**, 173106 (2012)

Snake states and Klein tunneling in a graphene Hall bar with a pn-junction

*Appl. Phys. Lett.* **100**, 163121 (2012)

Precision quantization of Hall resistance in transferred graphene

*Appl. Phys. Lett.* **100**, 164106 (2012)

Effect of e-beam irradiation on graphene layer grown by chemical vapor deposition

*J. Appl. Phys.* **111**, 084307 (2012)

Growth of triangle-shape graphene on Cu(111) surface

*Appl. Phys. Lett.* **100**, 163106 (2012)

---

### Additional information on *Appl. Phys. Lett.*

Journal Homepage: <http://apl.aip.org/>

Journal Information: [http://apl.aip.org/about/about\\_the\\_journal](http://apl.aip.org/about/about_the_journal)

Top downloads: [http://apl.aip.org/features/most\\_downloaded](http://apl.aip.org/features/most_downloaded)

Information for Authors: <http://apl.aip.org/authors>

## ADVERTISEMENT



**Goodfellow**  
metals • ceramics • polymers • composites  
70,000 products  
450 different materials  
**small quantities fast**

[www.goodfellowusa.com](http://www.goodfellowusa.com)

## Polarized light microscopy of chemical-vapor-deposition-grown graphene on copper

K. Kertész,<sup>1,2,a),b)</sup> A. A. Koós,<sup>3</sup> A. T. Murdock,<sup>3</sup> Z. Vértesy,<sup>1,2,b)</sup> P. Nemes-Incze,<sup>1,2,b)</sup> P. J. Szabó,<sup>4</sup> Z. E. Horváth,<sup>1,2,b)</sup> L. Tapasztó,<sup>1,2,b)</sup> Chanyong Hwang,<sup>2,5</sup> N. Grobert,<sup>3</sup> and L. P. Biró<sup>1,2,b)</sup>

<sup>1</sup>*Institute of Technical Physics and Materials Science, Centre for Natural Sciences, 1525 Budapest, P.O. Box 49, Hungary*

<sup>2</sup>*Korea-Hungary Joint Laboratory for Nanosciences, P.O. Box 49, 1525 Budapest, Hungary*

<sup>3</sup>*Department of Materials, University of Oxford, Oxford OX1 3PH, United Kingdom*

<sup>4</sup>*Department of Materials Science and Engineering, Faculty of Mechanical Engineering, Budapest University of Technology and Economics, P.O. Box 91, 1521 Budapest, Hungary*

<sup>5</sup>*Center for Advanced Instrumentation, Division of Industrial Metrology, Korea Research Institute of Standards and Science, Yuseong, Daejeon 305-340, South Korea*

(Received 22 March 2012; accepted 2 May 2012; published online 21 May 2012)

Linearly polarized light microscopy (PM) revealed that graphene grown by chemical vapor deposition (CVD) on stepped Cu substrate may appear colored. The coloration is associated with the coupling of the light of 450–600 nm into propagating mode in the graphene layer when the electric vector ( $\vec{E}$ ) of polarized light is parallel with the step edges and with the scattering when the  $\vec{E}$  is normal to the step edges. PM is an inexpensive, fast, and contamination free method to efficiently visualize graphene and to map the step structure of Cu substrates used for large area CVD growth of graphene. © 2012 American Institute of Physics. [<http://dx.doi.org/10.1063/1.4719205>]

Due to the very promising electronic, mechanical, and optical properties,<sup>1</sup> graphene has continuously been the focus of attention since it was first produced by mechanical cleavage.<sup>2</sup> At the beginning of the “graphene era,” mechanically cleaved graphene was made visible by optical microscopy.<sup>3</sup> This contributed significantly to the exponential development of the field (see Fig. 1 of Ref. 4). Optical methods based on polarized light are very versatile, even at submonolayer coverage.<sup>5,6</sup>

For practical applications, large area graphene must be produced at low cost. To achieve industrially viable prices, chemical vapor deposition (CVD) technique in conjunction with polycrystalline Cu substrates<sup>7</sup> is perhaps the best candidate to achieve these demands.<sup>8</sup> This process yields polycrystalline graphene material, i.e., a patchwork of randomly grown crystallites fused together.<sup>9</sup> The disorder of this patchwork originates from multiple sources, the most important being: random nucleation and the coalescence of the growing islands.<sup>10,11</sup> This leads to the formation of grain boundaries (GB)<sup>12–14</sup> that possess a different electronic structure than that of the graphene crystallites.<sup>15</sup> Therefore, nucleation control during the formation of the graphene crystallites<sup>16,17</sup> plays a crucial role in the creation of high-quality graphene. Another factor influencing material quality may be associated with nanoripples attributed to the step formation in the Cu substrate during graphene growth.<sup>18</sup>

Electron backscatter diffraction (EBSD) and Raman spectroscopy revealed that the growth on Cu(111) facets yields better quality graphene than on the Cu(100) facet.<sup>19</sup> Unfortunately, most commercial Cu foils produced by cold rolling exhibit a pronounced (100) texture.<sup>20</sup> On the (100)-textured surface of the Cu foils, four-lobed, 4-fold-symmet-

ric islands nucleate and grow.<sup>21</sup> Upon graphene formation the (100)-texture is maintained despite the fact that other facets are also observed.<sup>19</sup> As shown by scanning tunneling microscopy (STM), the graphene grown by this method is continuous over the prominent step structure which is generated during the graphene formation.<sup>22</sup> A further difference is found in the oxygen penetration under the graphene on different Cu facets. In contrast to Cu(111), on Cu(100) the oxygen penetrates beneath the graphene layer and oxidizes the Cu substrate.<sup>23</sup>

Optical characterization methods are extremely useful in order to investigate the orientation of individual Cu grains, their characteristic step structure,<sup>18</sup> and the graphene overlayer grown on them. Unlike scanning electron microscopy (SEM) and EBSD, they are contamination-free and easy to use.

Graphite is a birefringent material.<sup>24</sup> Recent experiments showed that in the case of linearly polarized light the light is coupled into propagating modes when  $\vec{E}$  oscillates in the graphene plane. However, when  $\vec{E}$  oscillates normal to the graphene plane the light is scattered in directions close to normal to the graphene plane.<sup>25</sup> Here we report the use of linearly polarized light in order to reveal the grain structure of the Cu substrate, and the orientation of the characteristic step structure formed during graphene growth<sup>21</sup> on the Cu crystallite facets with different Miller indices. Examining the samples with polarized light microscopy (PM) and offsetting the analyzer a few degrees from the rigorously crossed position with the polarizer, the graphene crystallites covering the Cu substrate appeared yellow or violet contrasting the homogeneous grey of the Cu substrate (Fig. 1). On the basis of spectrogoniometric and microspectrometric measurements we attribute these colors to the selective coupling of the polarized light with the graphene over the stepped surface of the Cu crystallites.

<sup>a)</sup>Electronic mail: [kertesz.krisztian@ttk.mta.hu](mailto:kertesz.krisztian@ttk.mta.hu).

<sup>b)</sup>URL: <http://www.nanotechnology.hu>.

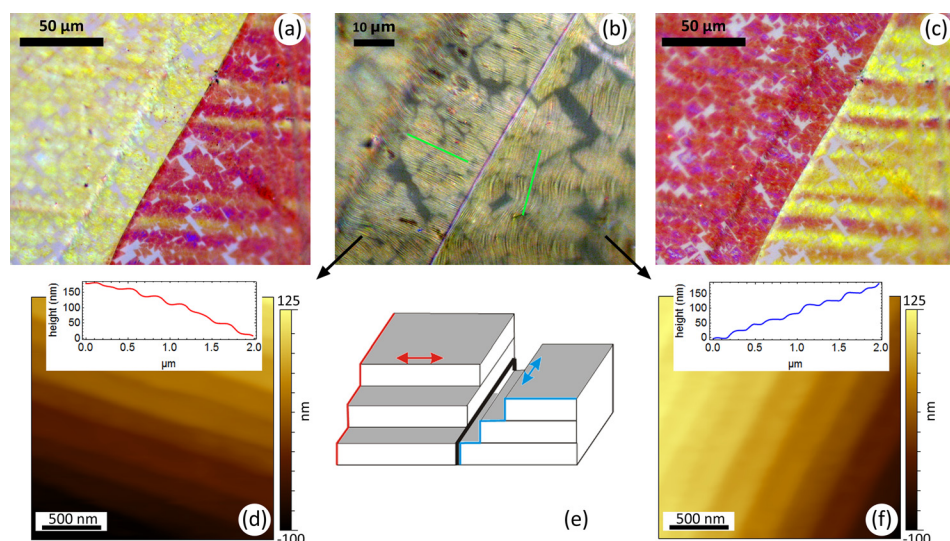


FIG. 1. Neighboring Cu grains with yellow/violet coloration and their characteristic step structure as revealed by PM and AFM images. (a), (c) yellow/violet and violet/yellow coloration at  $(90 + \Delta^\circ)$  and  $(90 - \Delta^\circ)$  setting of the analyzer; (b) high-resolution PM image with rigorously crossed polarizer and analyzer. Note the parallel steps in each grain. The green lines indicate the average step edge direction; (d), (f) contact mode AFM image of the two grains; (e) schematic presentations of the step structure in the two grains, the shaded faces are roughly parallel with the surface of the Cu foil.

Graphene was synthesized using low-pressure chemical vapor deposition of  $\text{CH}_4$  on Cu foils ( $25 \mu\text{m}$  thick; 99.999%; Alfa Aesar). The CVD set-up consisted of a quartz tube located inside a horizontal cylindrical furnace. The system was evacuated to a base pressure of  $<0.01$  Torr, purged with Ar, and backfilled with 500 sccm  $\text{H}_2$  at 4.1 Torr. The furnace was heated to  $1035^\circ\text{C}$  and the Cu substrates were then shifted into the hot zone of the furnace to anneal them in  $\text{H}_2$  for 60 min. Graphene was synthesized by adding 1 sccm  $\text{CH}_4$  for 10 min at 4.2 Torr. Subsequently, the  $\text{CH}_4$  was switched off, and the substrates were quenched by rapidly shifting them out of the hot zone in  $\text{H}_2$ .

The graphene grown on the Cu substrate was investigated by X-ray diffraction (XRD), PM in white light, SEM, EBSD, and various modes of atomic force microscopy (AFM) such as contact mode (C-AFM), friction force (FF-AFM), and conductive tip (CT-AFM) AFM. Detailed reflection spectra were acquired using a custom built spectromicroscope (SM) consisting of a Zeiss Axio Imager optical microscope combined with an Avantes fiber optic spectrometer, able to acquire microreflectivity data with a resolution of  $3 \mu\text{m}$ .<sup>26</sup>

In PM examination of a cubic metallic sample, like Cu,<sup>27</sup> increasing deviation from the rigorously crossed position of the polarizers will only increase the intensity of the transmitted light. Therefore it was quite surprising to observe that with close to crossed polarizers, graphene crystallites on neighboring Cu grains appear as violet and yellow colored patches (Fig. 1(a)). Furthermore, it was observed that the respective graphene crystallites switched color from violet to yellow and reverse when the analyzer position was changed from  $90 + \Delta^\circ$  to  $90 - \Delta^\circ$  (Fig. 1(c)). Here the deviation angle,  $\Delta$  is typically of the order of  $5^\circ$ – $10^\circ$ . This behavior was found to be characteristic for all the samples investigated in this work. High-resolution optical microscopy with rigorously crossed polarizers revealed a system of close to orthogonal striation on the two neighboring grains in Fig. 1 while graphene is barely visible as a pale yellow over the grey of Cu (Fig. 1(b)).

XRD confirmed the dominant (100) texture of the polycrystalline Cu foils after growth was completed. Cu grains exhibiting the above detailed color switching of the graphene

layer were typically found across the entire substrate surface. Detailed SEM and AFM investigations revealed (in agreement with optical microscopy studies) that the two neighboring grains of Fig. 1 possessed a well developed system of steps running close to parallel with each other within the same grain, and close to orthogonal to the steps in the neighboring grain (Fig. 1(b)). The AFM image in Fig. S2 (Ref. 27) shows that the region of the GB is not smooth. A schematic view of the step structure—omitting the few degrees inclinations in the region of the GB—is shown in Fig. 1(e). In Figs. 1(d) and 1(f) details of the step structure on the left and right hand side of the GB, respectively, are shown together with the corresponding AFM line-cuts.

Studies of an individual graphene flake in high-resolution using PM (Figs. 2(a) and 2(b)), topographic C-AFM (Fig. 2(c)), friction force measurements (Fig. 2(d)), CT-AFM, and SEM (Fig. S3 in Ref. 27), revealed that the violet or yellow coloration is not observed in those regions where the Cu surface is smooth. While PM clearly showed that in these regions the color is coincident with that of the Cu background (Fig. 2(a)), the AFM and SEM data convincingly showed that the graphene layer is present in these regions as well.

SM measurements performed on a single Cu grain with dense graphene coverage (all graphene crystallites exhibited the same coloration) in the spectral range from 400 to 700 nm revealed that when keeping the position of the polarizer and that of the analyzer fixed but rotating the sample a full  $360^\circ$  rotation around the sample normal, the color switching occurred four times, at positions offset from each other by  $90^\circ$  (Fig. 3(a)). The reference (see Ref. 27 for details) was chosen in an intermediate position between the yellow and violet colorations. In a complementary experiment the sample and the position of the polarizer was fixed. The analyzer was rotated from the crossed position to left ( $90 + \Delta^\circ$ ) and to right ( $90 - \Delta^\circ$ ). At each  $\Delta$  value a spectrum was recorded; the first four spectra are depicted in Fig. 3(b) (all spectra are shown in Ref. 27). As the  $\Delta$  value increased, the amount of light transmitted through the microspectrometer increased monotonically. However, for each  $+\Delta$  and  $-\Delta$  rotation of the analyzer a positive/negative plateau was found in the range of 450–600 nm, while the two

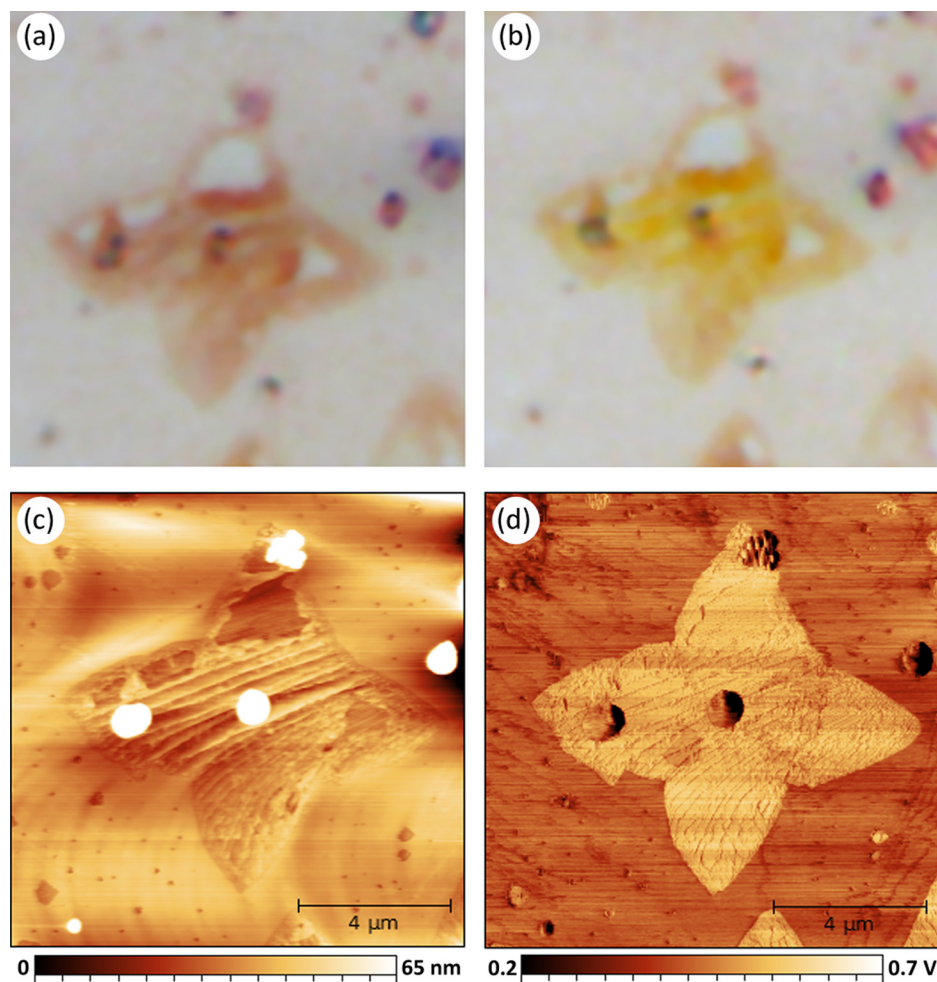


FIG. 2. PM and AFM images of an individual graphene flake. (a) PM image in violet and (b) yellow orientation, note certain regions where no color is observed. The same grey coloration can be observed as for the Cu background; (c) topographic C-AFM image; (d) FF-AFM image, note the characteristic difference between graphene and Cu.

curves—corresponding to  $+\Delta$  and  $-\Delta$ —ran close to each other in the wavelength ranges of 400–450 nm and 600–700 nm.

The graph shown in Fig. 4 was generated by plotting the difference between the reflection curves corresponding to  $+\Delta$  and  $-\Delta$  rotations of the analyzer measured at 500 nm as compared to the average reflectivity value measured at 700 nm. The color contrast was most pronounced at a few degrees from the rigorously crossed position, but at rigorously crossed polarizers there was no color contrast observed (see Figs. 1(b), too).

The linearly polarized light can have two distinct orientations with respect to the face of the Cu steps, which is in a plane at right angles with the plane of the Cu foil itself (see, Fig. 1(e), not shaded face), this will be called the “normal” face of the step, while the face parallel with the plane of the sample (shaded face) will be called the “parallel” face of the step. Light with the  $\vec{E}$  parallel with the normal face may be coupled into the graphene membrane covering the normal face of the step.<sup>25</sup> It will be reflected/scattered at the bottom of the step under angles close to the incidence angle so that a significant fraction will enter the microscope objective. On the contrary, the light with  $\vec{E}$  perpendicular to the normal face of the step will be scattered close to angles normal to this step face<sup>25</sup> so that most of it will be lost and not captured by the microscope objective. These processes will be responsible for the “additional” light in the spectral range of 400–650 nm, causing the yellow color when the plane of

polarization is parallel with the normal face of the step. The lack of the light scattered so that it cannot enter the microscope objective will cause the violet color when the plane of polarization is normal to the normal step face. Under a full circle rotation there will be two yellow and two violet positions at  $180^\circ$  from each other for each system of steps. The two positions for light coupling into the graphene overlaying the normal step faces are shown in Fig. 1(e) by double arrows: red for one step orientation and blue for the orthogonal step orientation. For intermediate positions between parallel and perpendicular orientation of the polarization plane with respect to the normal step face, one can decompose the electric field vector  $\vec{E}$  into a parallel and a normal component. This reduces the discussion to the two cases discussed above. The same is valid for the case when the “normal” step face may have some deviation from the rigorously normal orientation with respect to the sample surface. On a more general level the decomposition of the  $\vec{E}$  into components parallel and normal to the graphene surface is justified in any region where the surface is corrugated. A completely random corrugation or a smooth surface is not expected to yield a marked color contrast—as it will lack the preferential orientation arising from close to parallel steps—while a regularly corrugated structure like the step systems in Fig. 1 clearly will yield color contrast.

Another important point may be that when individual graphene flakes grow together to form a continuous layer on

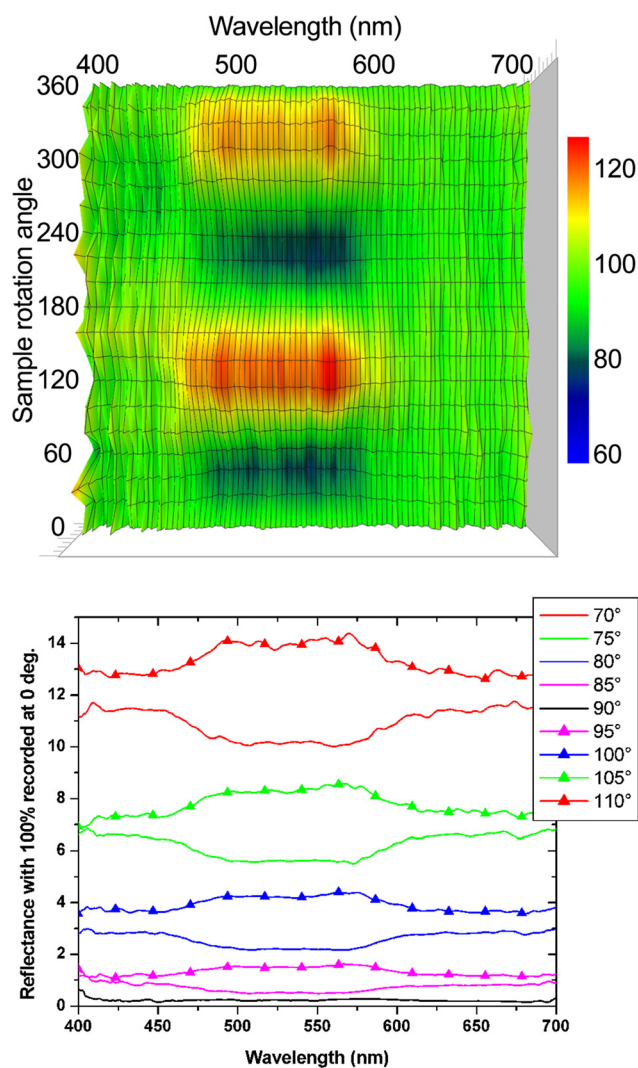


FIG. 3. Intensity of linearly polarized light reflected from graphene over the same Cu grain as measured by microspectrometer. (a) Color changes with slightly off-crossed polarizers as the sample was rotated on the stage of the microspectrometer, the color code on right hand side indicated the intensity of the reflected light (100 correspond to color neutrality). (b) Color of the same Cu grain in  $(90 + \Delta)^\circ$  and  $(90 - \Delta)^\circ$  positions as  $\Delta$  is increased from  $0^\circ$  to  $20^\circ$ .

the surface of the polycrystalline Cu foil, each Cu crystallite may have a characteristic step topography (different from the step topography of the neighbors; see for example Fig. 1(e)), which will be “frozen” in the structure of the graphene overlayer. Even after transferring this graphene overlayer onto an atomically flat surface, wrinkles will continue to be present and to generate mechanical stresses in the graphene. This mechanical stress in turn may alter both electronic and the optical properties of graphene.<sup>18,28</sup> An additional advantage of the use of PM is that it allows the quick and simple investigation of Cu grain step structures—which may be indicative of the copper grain orientation—without the need of using SEM and EBSD which inherently contaminate the scanned surface with amorphous carbon. Such a layer of amorphous deposit would be highly undesirable.

To check for possible effects not related to the step structure of the Cu substrate, graphene flakes were transferred from the Cu substrate to  $\text{SiO}_2/\text{Si}$  surface ( $\text{SiO}_2$  thickness 90 nm); the graphene crystallites did not exhibit any color

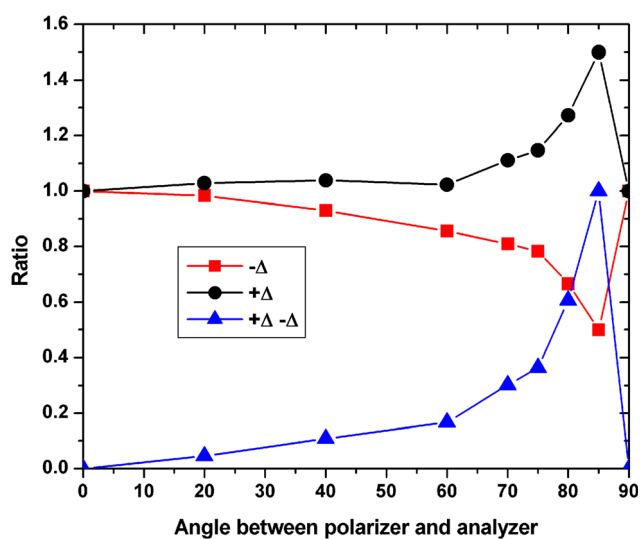


FIG. 4. Ratio of reflected light intensities as in Fig. 3(b):  $(I_{+\Delta} - I_{\text{average}})/I_{\text{average}}$  (black curve),  $(I_{\text{average}} - I_{-\Delta})/I_{\text{average}}$  (red curve), and  $(I_{+\Delta} - I_{-\Delta})/I_{\text{average}}$  (blue curve) as  $\Delta$  increases from  $0^\circ$  to  $90^\circ$ . One may note that the color contrast is reduced as the analyzer approaches the parallel position with the polarizer.

change in non-polarized or polarized light; their coloration was slightly darker blue as compared with the substrate.<sup>27</sup>

Polarized light microscopy proved to be a useful tool in the fast, large area, and contamination free investigation of the characteristic step structure developed on polycrystalline Cu used as a substrate for CVD graphene. The yellow/violet coloration of graphene covered Cu grains when observed in linearly polarized light is attributed to the coupling of light in the spectral range from 450 to 600 nm into a propagating mode in the graphene layer, while light with  $\vec{E}$  normal to the step edges is scattered.

This work has been conducted within the framework of the Korean-Hungarian Joint Laboratory for Nanosciences (KHJLN), the Converging Research Center Program through the Ministry of Education, Science and Technology (2010K000980), OTKA grant PD 84244 and K 101599. We are grateful to the Royal Society (NG), the European Research Council (ERC-2009-StG-240500) (NG), the Engineering and Physical Sciences Research Council Pathways to Impact Awards (NG), and the Clarendon and Commonwealth Scholarships (ATM).

<sup>1</sup>A. K. Geim, *Science* **324**, 1530–1534 (2009).

<sup>2</sup>K. S. Novoselov, A. K. Geim, S. V. Morozov, D. Jiang, Y. Zhang, S. V. Dubonos, I. V. Grigorieva, and A. A. Firsov, *Science* **306**, 666–669 (2004).

<sup>3</sup>P. Blake, E. W. Hill, A. H. C. Neto, K. S. Novoselov, D. Jiang, R. Yang, T. J. Booth, and A. K. Geim, *Appl. Phys. Lett.* **91**, 063124 (2007).

<sup>4</sup>L. P. Biró, P. Nemes-Incze, and P. Lambin, *Nanoscale* **4**, 1824–1839 (2012).

<sup>5</sup>H. H. Rotermund, G. Haas, R. U. Franz, R. M. Tromp, and G. Ertl, *Science* **270**, 608–610 (1995).

<sup>6</sup>J. Dicke, H.-H. Rothermund, and J. Lauterbach, *J. Opt. Soc. Am.* **17**, 135–141 (2000).

<sup>7</sup>X. Li, W. Cai, J. An, S. Kim, J. Nah, D. Yang, R. Piner, A. Velamakanni, I. Jung, E. Tutuc, S. K. Banerjee, L. Colombo, and R. S. Ruoff, *Science* **324**, 1312–1314 (2009).

<sup>8</sup>S. Bae, H. Kim, Y. Lee, X. Xu, J.-S. Park, Y. Zheng, J. Balakrishnan, T. Lei, H. R. Kim, Y. I. Song, Y.-J. Kim, K. S. Kim, B. Ozyilmaz, J.-H. Ahn, B. H. Hong, and S. Iijima, *Nat. Nanotechnol.* **5**, 574–578 (2010).

<sup>9</sup>B. I. Yakobson and F. Ding, *ACS Nano* **5**, 1569–1574 (2011).

- <sup>10</sup>X. Li, C. W. Magnuson, A. Venugopal, J. An, J. W. Suk, B. Han, M. Borysiak, W. Cai, A. Velamakanni, Y. Zhu, L. Fu, E. M. Vogel, E. Voelkl, L. Colombo, and R. S. Ruoff, *Nano Lett.* **10**, 4328–4334 (2010).
- <sup>11</sup>C. Hwang, K. Yoo, S. Kim, E. Seo, H. Yu, and L. P. Biro, *J. Phys. Chem. C* **115**, 22369–22374 (2011).
- <sup>12</sup>P. Y. Huang, C. S. Ruiz-Vargas, A. M. van der Zande, W. S. Whitney, M. P. Levendorf, J. W. Kevek, S. Garg, J. S. Alden, C. J. Hustedt, Y. Zhu, J. Park, P. L. McEuen, and D. A. Muller, *Nature (London)* **469**, 389–392 (2011).
- <sup>13</sup>A. Mesáros, S. Papanikolaou, C. Flipse, D. Sadri, and J. Zaanen, *Phys. Rev. B* **82**, 205119 (2010).
- <sup>14</sup>P. Nemes-Incze, K. J. Yoo, L. Tapasztó, G. Dobrik, J. Lábár, Z. E. Horváth, C. Hwang, and L. P. Biró, *Appl. Phys. Lett.* **99**, 023104 (2011).
- <sup>15</sup>L. Tapasztó, P. Nemes-Incze, G. Dobrik, K. J. Yoo, C. Hwang, and L. P. Biró, *Appl. Phys. Lett.* **100**, 053114 (2012).
- <sup>16</sup>H. Wang, G. Wang, P. Bao, S. Yang, W. Zhu, X. Xie, and W.-J. Zhang, *J. Am. Chem. Soc.* **134**, 3627–3630 (2012).
- <sup>17</sup>Q. Yu, L. A. Jauregui, W. Wu, R. Colby, J. Tian, Z. Su, H. Cao, Z. Liu, D. Pandey, D. Wei, T. F. Chung, P. Peng, N. P. Guisinger, E. A. Stach, J. Bao, S.-S. Pei, and Y. P. Chen, *Nat. Mater.* **10**, 443–449 (2011).
- <sup>18</sup>G.-X. Ni, Y. Zheng, S. Bae, H. R. Kim, A. Pachoud, Y. S. Kim, C.-L. Tan, D. Im, J.-H. Ahn, B. H. Hong, and B. Ozyilmaz, *ACS Nano* **6**, 1158–1164 (2012).
- <sup>19</sup>J. D. Wood, S. W. Schmucker, A. S. Lyons, E. Pop, and J. W. Lyding, *Nano Lett.* **11**, 4547–4554 (2011).
- <sup>20</sup>A. Okada, H. Mitsui, and H. Nakaé, *Proc. Jpn. Inst. Met.* **15**, 417–422 (1974).
- <sup>21</sup>J. M. Wofford, S. Nie, K. F. McCarty, N. C. Bartelt, and O. D. Dubon, *Nano Lett.* **10**, 4890–4896 (2010).
- <sup>22</sup>H. I. Rasool, E. B. Song, M. J. Allen, J. K. Wassei, R. B. Kaner, K. L. Wang, B. H. Weiller, and J. K. Gimzewski, *Nano Lett.* **11**, 251–256 (2011).
- <sup>23</sup>A. Walter, S. Nie, A. Bostwick, K. S. Kim, L. Moreschini, Y. J. Chang, D. Innocenti, K. Horn, K. McCarty, and E. Rotenberg, *Phys. Rev. B* **84**, 195443 (2011).
- <sup>24</sup>S. Ergun, *Nature (London)* **213**, 135–136 (1967).
- <sup>25</sup>Q. Bao, H. Zhang, B. Wang, Z. Ni, C. H.Y. X. Lim, Y. Wang, D.Y. Tang, and K.P. Loh, *Nature Photonics* **5**, 411–415 (2011).
- <sup>26</sup>K. Kertész, Z. Bálint, Z. Vártesy, G. Márk, V. Lousse, J. Vigneron, M. Rassart, and L. P. Biró, *Phys. Rev. E* **74**, 021922 (2006).
- <sup>27</sup>See supplementary material at <http://dx.doi.org/10.1063/1.4719205> for polarized light microscopy of Cu foil, for AFM details, for SM details, and for transferred graphene microscopy
- <sup>28</sup>T. Jiang, D. Emerson, K. Twarowski, D. Finkenstadt, and J. Therrien, *Phys. Rev. B* **82**, 235430 (2010).